ECS Transactions, 3 (10) 315-324 (2006)
10.1149/1.2357272, copyright The Electrochemical Society

Diamond/Carbon Field Emission Based Structures for Sensors and MEMS

J. L. Davidson, W. P. Kang, Y. M. Wong, and K. Subramanian.
Department of Electrical Engineering and Computer Science,
Vanderbilt University, Nashville, TN 37235, USA.

Chemical vapor deposited diamond/carbon micro- and nanostructures are excellent field emission cathodes for novel applications in sensors, MEMS, and NEMS because of their low electron affinity and excellent mechanical and chemical properties. However, practical micropatterning and fabrication of emitter structures are needed to fully exploit their potential use. This paper describes the use of microfabrication methods to achieve various forms of morphologically-engineered cathodes such as micro pyramidal tips with self-aligned gated membrane, nano-diamond lateral field emitters with built-in anode, and carbon-nanotube field emission arrays with self-aligned gate. We report the achievement of these micropatterned diamond/carbon field emission-based sensing platforms with excellent field emission characteristics. These field emitter-based microstructures are efficient sensing platforms from which novel sensors and MEMS can be derived.

I. Introduction

We will discuss 3 types of carbon based cold cathode electron sources. 1) Diamond field emission cathodes with self-aligned gate membrane which were fabricated from a silicon-on-insulator substrate (SOI). This fabrication technique utilizes conventional silicon micropatterning and etching techniques to define the gate, and cathode. The fabrication has achieved gated diamond field emitters over practical wafer areas. The field emission of the gated arrays exhibits stable emission characteristics. 2) Nanodiamond lateral field emitters which were fabricated on a SOI substrate using a single-mask process. 3) We also present the development of self-aligned gated carbon nanotubes (CNTs) for cold cathode based sensing applications. Vertically aligned CNTs were used to form a microcathode with a convex surface profile, being selectively synthesized from microwave plasma chemical vapor deposition (MPCVD) with sputtered Ni or Co as catalyst for CNTs synthesis.

II. Fabrication

Fabrication of Diamond Pyramidal Tips and Edge Emitters

The fabrication steps for diamond pyramidal tips (1,2) and edge emitters (3) are shown in Fig. 1. The Si wafer was 500 μm thick. A 0.2 μm thick oxide was then grown on the wafer surfaces. Inverted pyramidal cavities were then etched into the Si substrate using photolithographic patterning and anisotropic etching of silicon with KOH solution. Next a SiO_2 layer was grown into the mold to produce a well-sharpened apex in the inverted pyramidal cavity. Diamond was then grown into the mold using MPCVD. The MPCVD parameters were controlled so as to achieve small but deliberate sp^2 content in the diamond film. Next the back-side silicon and SiO_2 was etched away and sharpened diamond pyramidal geometries exposed for non-gated diamond emitters. In the case of

gated diamond emitters, a square window was opened on the backside of the silicon mold and the silicon was then anisotropically etched until the apex of SiO_2 covered diamond pyramids were exposed. Ethylenediamine based (EDP) etching solution was used for the controlled silicon anisotropic etching. Finally, the SiO_2 near the apex region was etched away to expose the naturally sharpened diamond tips. The remaining SiO_2 and silicon form the dielectric spacer and the gate, respectively. The diamond film was characterized using scanning electron microscopy (SEM) and Raman spectroscopy. The SEM image of an array of diamond pyramidal tips and edge emitters is shown in Fig. 2 and 3, respectively. The tips had a base dimension of 12 μm x 12 μm, while the edges had a width of 2 μm and length of 125 μm. A SEM of the vertical diamond field emission triode is shown in Fig. 4. The fabricated diamond emitter has a very sharp apex (~5 nm), surrounded by a self-aligned silicon gate. The diamond cathode is electrically insulated from silicon gate by a 2 μm thick SiO_2 layer.

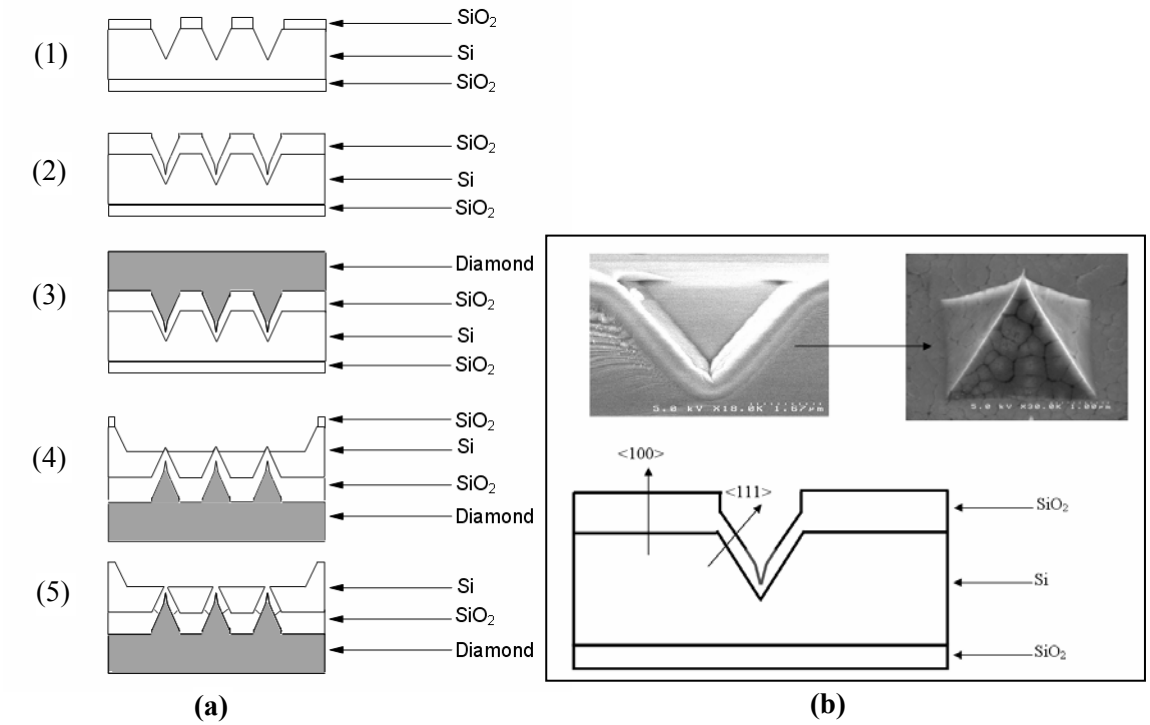

Fig.1. (a) Fabrication steps for sharpened diamond tips and self-aligned gated diamond tips, and (b) SEM micrograph of a single sharpened silicon mold, a single sharpened diamond tip and the corresponding schematic cross-section.

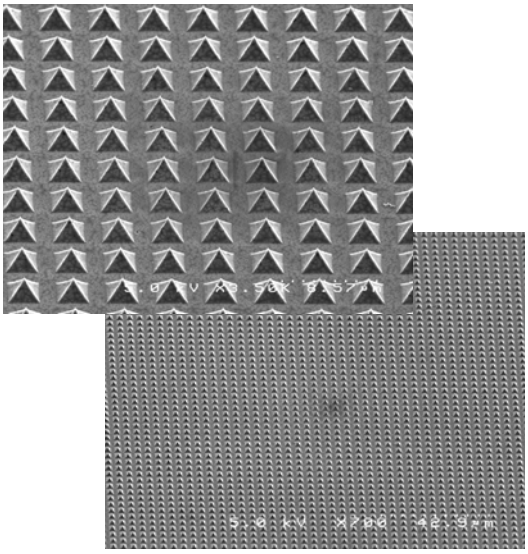

Fig.2. SEM high-density diamond tips array

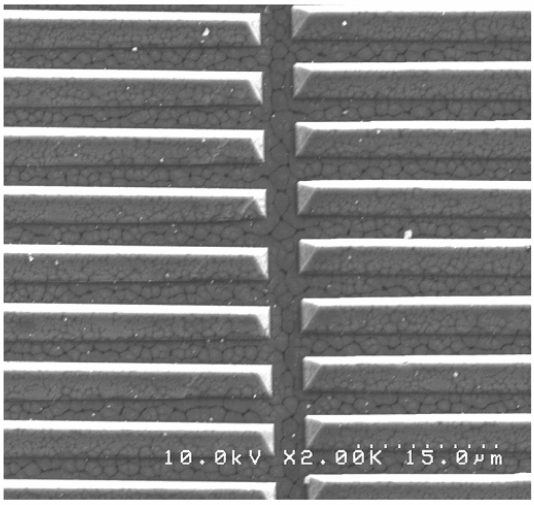

Fig.3. SEM of diamond edge array

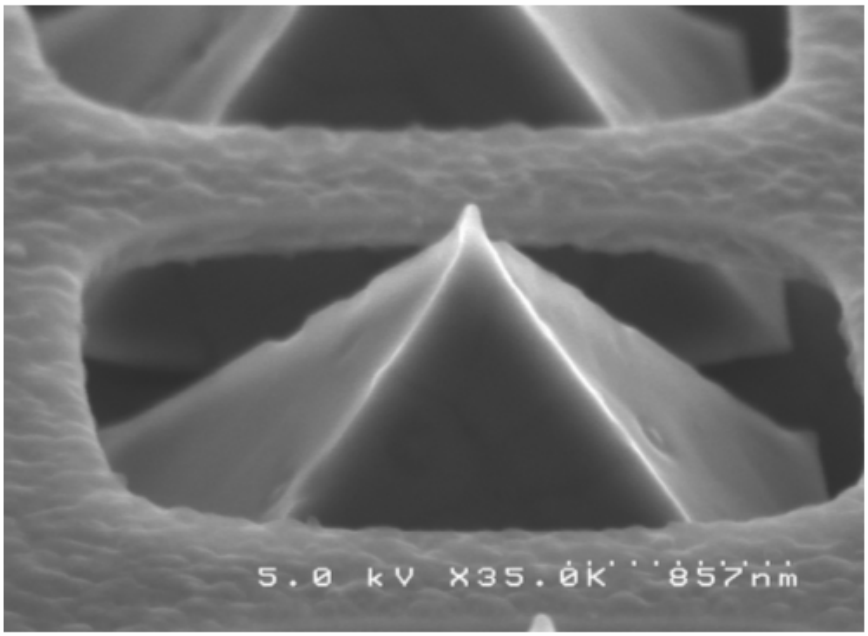

Fig.4. SEM of a self-aligned gated diamond field emitter

Fabrication of Lateral Diamond Field Emission Arrays

Fabrication of lateral diamond field emission arrays with co-built anode - The fabrication flow chart of the lateral diamond field emitter array with co-built anode is shown in Fig. 5. Nanodiamond (ND) lateral field emitters are fabricated on a SOI substrate using a single-mask process (4). The fabrication begins with the growth of a 2-µm thick ND film on a SOI wafer. ND films with grain size of 5-10 nm were achieved in an MPCVD system using a gas mixture of $CH_4/H_2/N_2$, employing growth-rate reduction conditions. Next, an aluminum metal layer was deposited by thermal evaporation. The aluminum layer was then patterned with the lateral anode and cathode patterns using

photolithography. With this aluminum serving as a mask, patterning of the nanodiamond film was carried out with RIE using pure oxygen plasma (5). Subsequent silicon etching was performed using a RIE system and a SF_6/O_2 plasma to achieve isolation between the nanodiamond electrodes and set the anode–cathode spacing. Figure 6 is an SEM image of lateral ND field emitters with the silicon support partially etched away. The anode-cathode spacing can be designed for any length per a specific sensor or MEMS design.

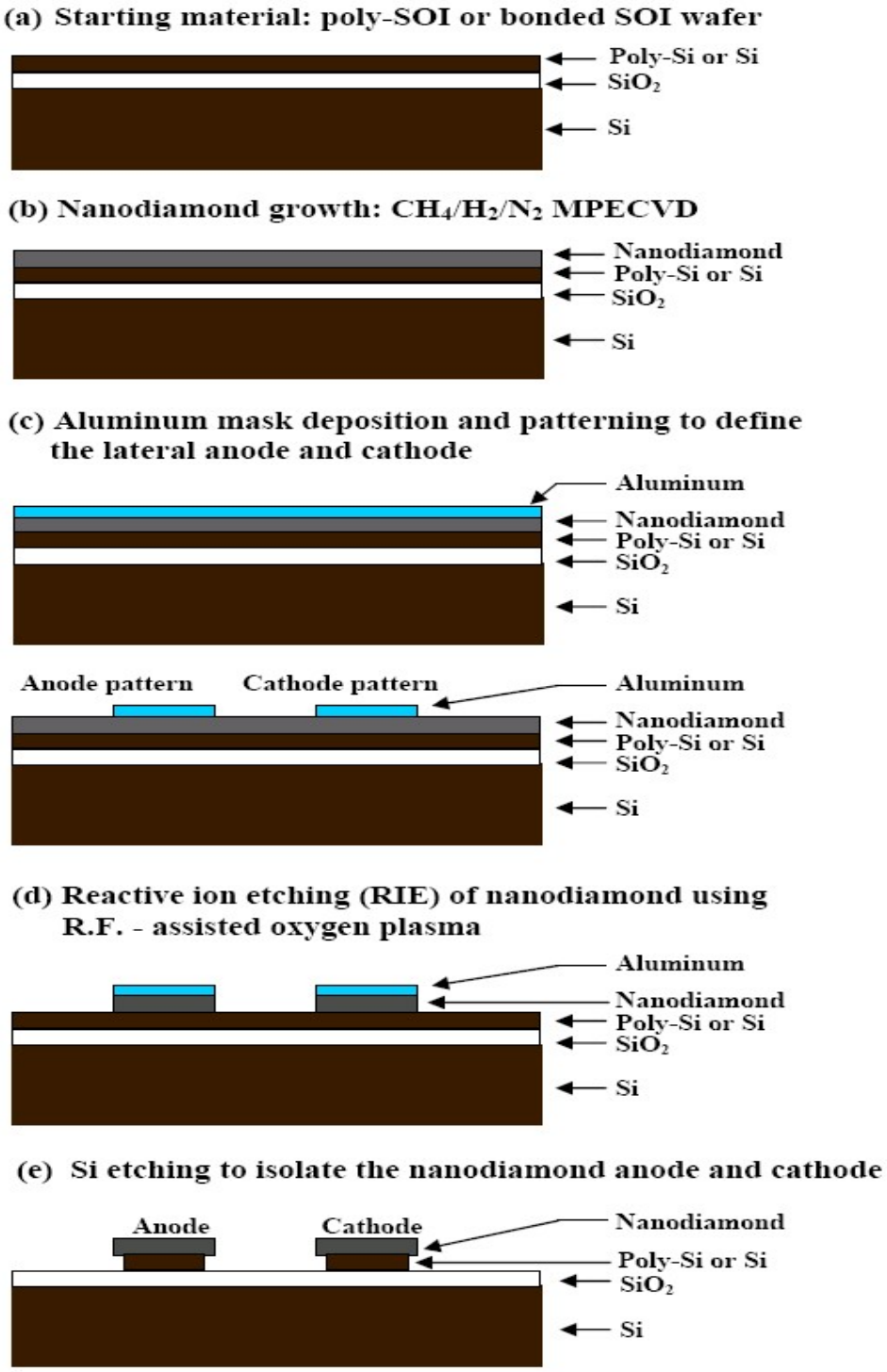

Fig. 5. Fabrication flow chart of the lateral diamond field emitter array

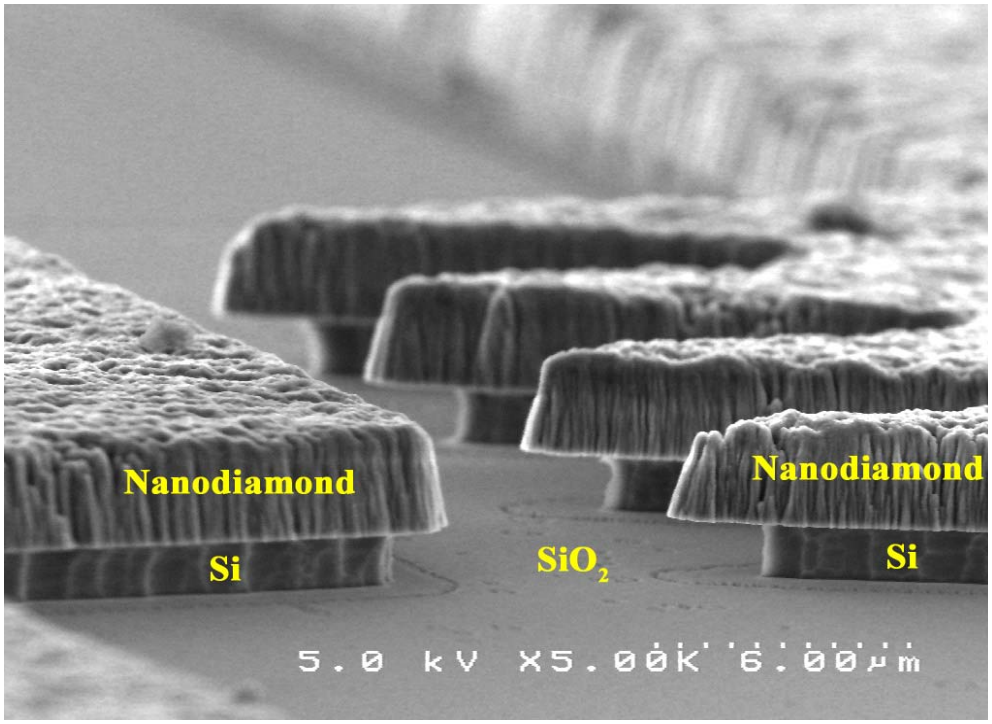

Fig. 6. SEM of lateral ND field emitters

Fabrication of Gated Carbon Nanotubes Field Emission Arrays

We also developed self-aligned gated CNTs for cold cathode based sensing applications. Vertically aligned CNTs were used to form a microcathode with a convex surface profile, being selectively synthesized from MPCVD with sputtered Ni or Co as catalyst for CNTs synthesis. The convex profile of the gated CNT emitter is important in the prevention of cathode-gate leakage without resorting to more complex fabrication processes such as (i) over-etched gate electrode or reduced gate overhang (6,7), (ii) sidewall protector (8-11), and (iii) post-growth processing which includes utilizing chemical mechanical polishing (CMP) technique (12), or plasma trimming of the grown CNTs (13).

The single-mask microfabrication process achieved an array of 10 µm x 10 µm CNT microtriodes with 2856 array cells and 20 µm array spacing. As illustrated in the schematic fabrication process in Fig. 7, the process began with a low-pressure CVD deposition of polysilicon as the gate electrode on thermally oxidized highly doped n-type silicon (100) substrate. A spin-on-diffusion source was utilized to dope the polysilicon gate at high-temperature (1050 ºC) for good conductivity. The thickness of the thermal oxide and the polysilicon gate layers was ~ 1.5 µm and 0.8 µm, respectively.

After conventional photolithography patterning, the polysilicon gate was subsequently dry-etched by a gas mixture of sulfur hexafluoride (SF_6) and oxygen (O_2) at 150 mTorr in a reactive-ion-etch system (MRC). Next, the thermal oxide was isotropically wet-etched with buffered-oxide-etch (BOE) to obtain an undercut structure

as illustrated in Fig. 8. The appeared "two" polysilicon layers may due to incomplete diffusion of doping source (step 1 in Fig. 7) and different etching rate of the two layers when subjected to RIE (step 2). A thin film of titanium (Ti) ~20 nm, a diffusion barrier layer and Ni ~ 5-10 nm, acting as nanocluster catalytic centers for CNT nucleation growth catalyst, were sputter deposited in sequence using a DC magnetron sputtering system (MRC) on the triode sample without breaking the vacuum. The surplus catalyst on the polysilicon gate was removed utilizing photoresist lift-off technique by acetone.

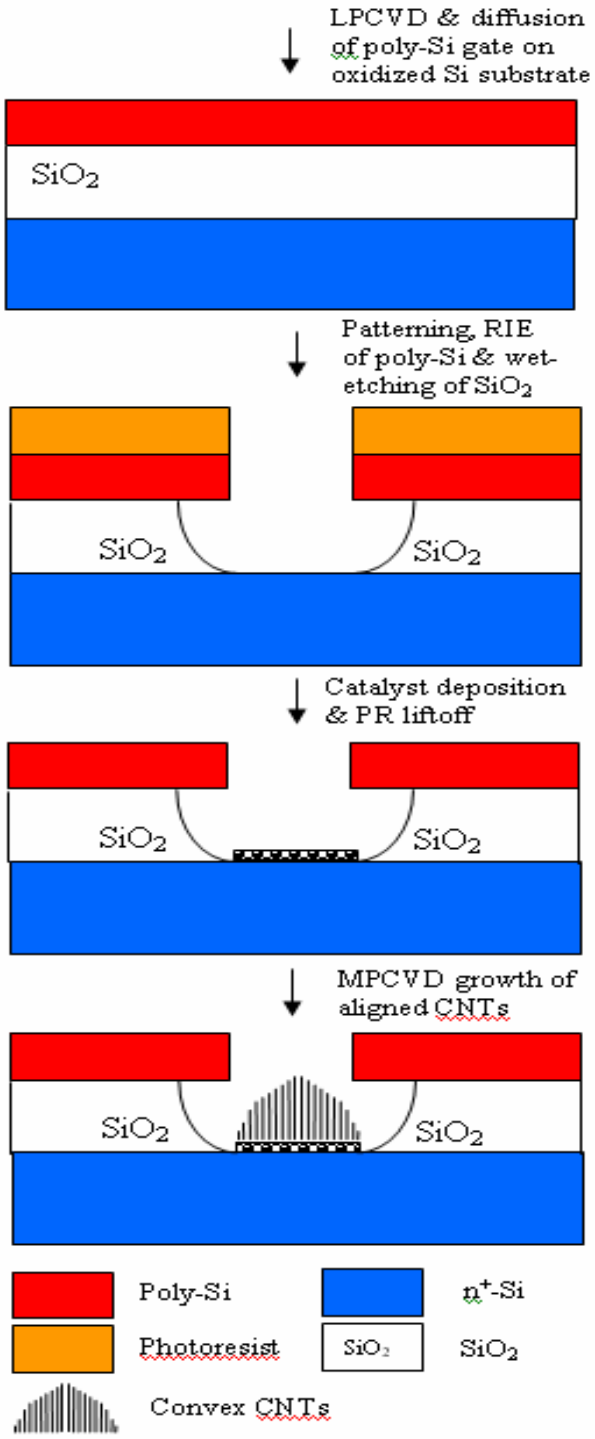

Fig. 7. Schematic diagrams of the single-mask fabrication process for the CNT emitters.

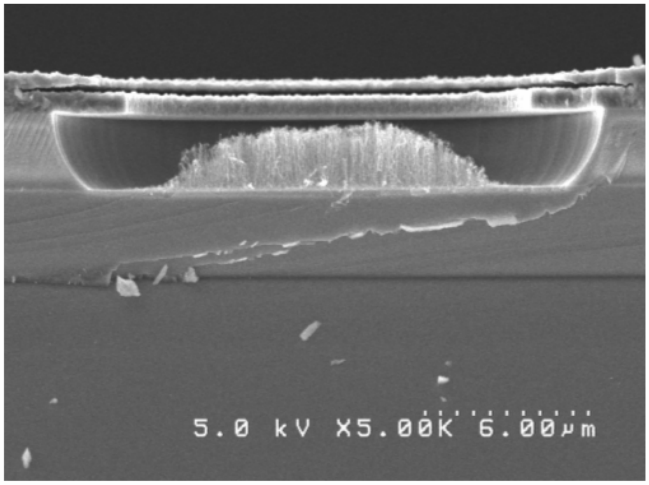

Fig. 8. SEM micrograph of the gated CNTs emitter.

The MPCVD system used to grow aligned CNTs in this study is an ASTeX 1.5 kW microwave plasma system equipped with an *RF* induction heater for substrate heating. The same system has been routinely used to synthesize polycrystalline and nanocrystalline diamonds by adopting different growth parameters (14-16). The triode sample was then transferred to the CVD chamber and heated to 400 ^{o}C in flowing H_2 with a working pressure of 20 Torr. A critical H_2 plasma pretreatment of the catalysts at microwave power of 400 W was performed for a specified duration of time. Note that this pre-growth catalyst pretreatment is important in obtaining the required convex-shaped cathode structure.

After the pretreatment, the substrate temperature was raised to 650 ^{o}C, the synthesis temperature. Upon reaching the particular temperature, CH_4 gas and microwave power of 1 kW was applied instantly to initiate the CNTs growth for ~60-90 s. The specified growth time was critical to obtain the optimum height of the vertically aligned CNT cathodes without cathode-gate shorting. The flow ratio of the gas mixtures, CH_4:H_2 was maintained at 1:8 with a total flowrate of 135 sccm during the CNTs growth.

III. Electrical Characterization

The fabricated diamond emission diodes and triodes were tested for electron emission under vacuum at 10^{-6} Torr. The emission current was recorded as a function of applied voltages. Fowler-Nordheim (F-N) equation was used to analyze the diamond field emission data:

$$\ln(I/E^2) = \ln(A*K_1*\beta^2/\Phi) - (K_2*\Phi^{1.5}/\beta)(1/E) \qquad [1]$$

where K_1 and K_2 are constants : $K_1 = 1.54 \times 10^{-6}$ AeV/V^2, $K_2 = 6.83 \times 10^7$ V/(cm eV$^{3/2}$), I is the emission current, Φ is the work function of the emitting surface in eV, β is the geometrical field enhancement factor, A is the emitting area, and E is the applied electric field.

A mica spacer 120 μm thick provided the cathode-anode gap. Emission measurements at various temperatures were performed after the vacuum stabilized at 10^{-6} Torr. The current-voltage behavior was recorded to a computer interfaced with the test chamber. Fig. 9 (inset) demonstrates that the emission current of this diamond diode conforms to F-N behavior. The electron emission characteristics, anode emission current versus anode voltage (I_a-V_a plots), of a self aligned gated diamond triode for various gate voltages (V_g) are reported elsewhere (17). The diamond field emission triode provides a high voltage gain when operated as an amplifier and is a very promising prospect for signal amplification applications.

The emission characteristic of a lateral diamond field emission diode is shown in Fig.10. The figure shows that the lateral diamond field emitter has a very low turn-on voltage of ~5 V and a high emission current of 6 μA, from the four diamond fingers, at an anode voltage of 25 V. The anode-cathode spacing is ~2 μm. Thus, the lateral field emitter exhibits a very low turn-on field of ~3 V/μm, which is the lowest reported value for lateral field emitters (18-20). Inset of Fig. 10 shows the corresponding F-N plot for lateral field emitter. The linearity of this plot confirms the observed current originate from electron field emission.

Finally, electron emission results, Fig. 11, demonstrate that CNTs configured as field emitters exhibit low turn-on voltage of ~25 V, which compared favorably to other reported results (7-13). More importantly, high emission current with low gate leakage or interception current of less than 10% of the anode current was achieved.

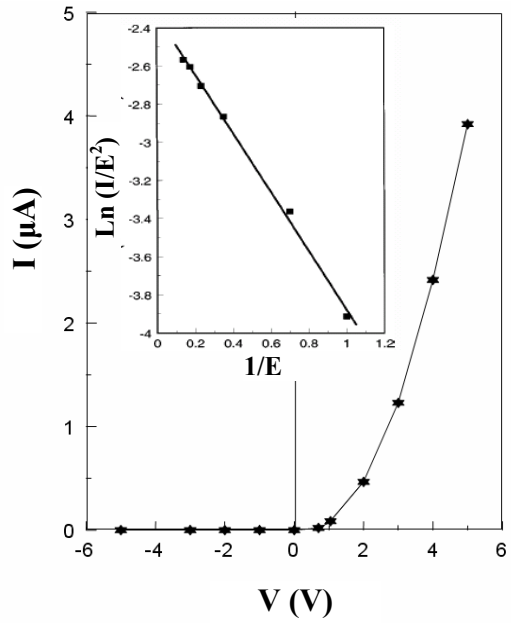

Fig. 9. Emission characteristics of vertically configured diamond diode.

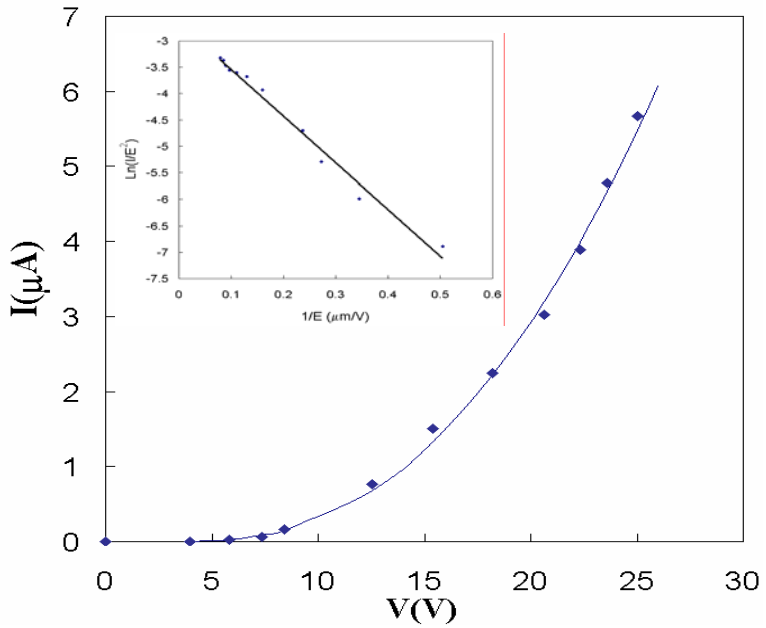

Fig. 10. Emission characteristics of lateral diamond field emission diode.

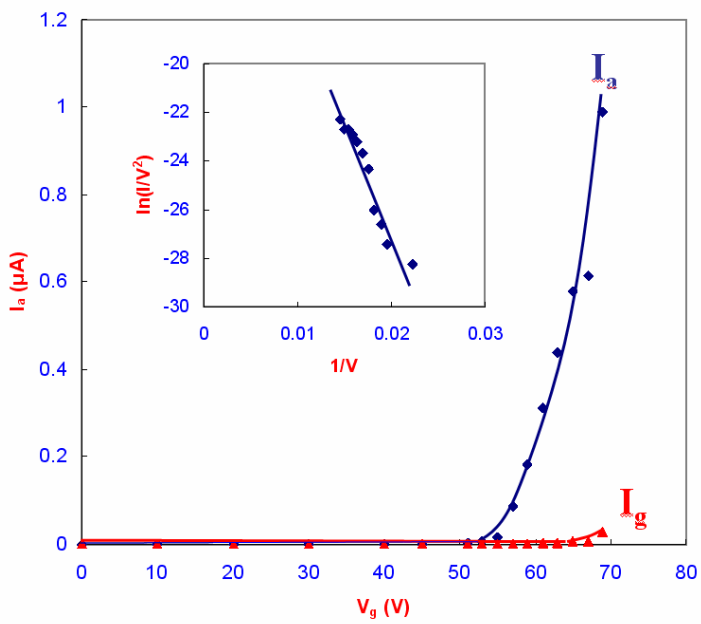

Fig. 11. Emission characteristics of the CNT gated emitter.

IV. Summary

In summary, diamond and carbon nanotube field emission devices have been developed and their vacuum electron emission behavior examined. These microstructures present a robust platform from which numerous electronic and bio-chemical sensors are being derived.

References

1. A. Wisitsora-at, W. P. Kang, J. L. Davidson, and D. V. Kerns, *Appl. Phys. Lett.*, **71**, 3394 (1997).
2. W. P. Kang, A. Wisitsora-at, J. L. Davidson, M. Howell, D. V. Kerns, Q. Li, J. F. Xu, and C. K. Kim, *J. Vac. Sci. Technol. B*, **16**, 732 (1998).
3. R.S. Takalkar, J.L. Davidson, W.P. Kang and A. Wisitsora-at, *Diamond Relat. Mater.*, **14**, 692 (2005).
4. K. Subramanian, W.P. Kang, J.L. Davidson, W.H. Hofmeister, B.K. Choi, and M. Howell, *J. Vac. Sci. Technol. B*, **24**, 953 (2006).
5. K. Subramanian, W.P. Kang, J.L. Davidson, W.H. Hofmeister, B.K. Choi, and M. Howell, *Diamond Relat. Mater.*, **14**, 2099 (2005).
6. Y. M. Wong, W. P. Kang, J. L. Davidson, W. Hofmeister, S. Wei, and J. H. Huang, *J. Vac. Sci. Technol. B*, **23**, 868 (2005).
7. K. J. Chen, W. K. Hong, C. P. Lin, K. H. Chen, L. C. Chen, and H. C. Cheng, *IEEE Electron Device Lett.*, **22**, 516 (2001).
8. S. D. Ahn, Y. H. Song, S. Y. Choi, J. B. Park, J. I. Sohn, S. H. Lee, J. H. Lee, K. I. Cho, *Proceedings of the 14th International Vacuum Microelectronics Conference IEEE*, p. 55, Davis, CA (2001).
9. Y. Huh, J. Y. Lee, J. H. Lee, T. J. Lee, S. C. Lyu and C. J. Lee, *Chem. Phys. Lett.*, **375**, 388 (2003).
10. Y. Y. Jang, C. H. Choi, B. K. Ju, J. H. Ahn, and Y. H. Lee, *Thin Solid Films*, **436**, 298 (2003).
11. D. S. Y. Hsu, *Appl. Phys. Lett.*, **80**, 2988 (2002).
12. W.J. Yu, Y.S. Cho, G.S. Choi, D.J. Kim, Y.H. Song, and J.H. Lee, *Diamond Relat. Mater.*, **13**, 1017 (2004).
13. S. Kang, C. Bae, W. Son, M. H. Kim, J. Yi, A. Chang, J. J. Kim, and C. R. Lee, *Technical Digest of the 16th International Vacuum Microelectronics Conference IEEE*, p. 51, Osaka, Japan (2003).
14. W.P. Kang, J.L. Davidson, A. Wisitsora-at, Y.M. Wong, R. Takalkar, K. Subramanian, D.V. Kerns and W.H. Hofmeister, *Diamond Relat. Mater.*, **14**, 685 (2005).
15. A. Wisitsora-at, W. P. Kang, J. L. Davidson, M. Howell, W. Hofmeister, and D. V. Kerns, *J. Vac. Sci. Technol. B*, **21**, 1671 (2003).
16. W. P. Kang, J. L. Davidson, Y. M. Wong and K. Holmes, *Diamond Relat. Mater.,* **13**, 975 (2004).
17. A. Wisitsora-at, W. P. Kang, J. L. Davidson, Y. Gurbuz, and D.V. Kerns, *Diamond Relat. Mater.*, **8**, 1220 (1999).
18. C. S. Lee, J. D. Lee, and C. H. Han, *IEEE Electron Devices Lett.*, **21**, 479 (2000).
19. M. Y. A. Turner, R. J. Roedel, and M. N. Kozicki, *J. Vac. Sci. Technol. B,* **17**, 1561 (1999).
20. S. S. Park, D. I. Park, S. H. Hahm, J. H. Lee, H. C. Choi, and J. H. Lee, *IEEE Trans. Electron Devices*, **46**, 1283 (1999).